

# Electroactive Microbes

ε-machines as environmental signal generators

Patrick Beckett

Department of Civil and Environmental Engineering

[pbeckett@ucdavis.edu](mailto:pbeckett@ucdavis.edu)

**Abstract:** Electroactive bacteria are a group of microorganisms with unique physiological features related to their electron transport chains, and often form multi-cellular conductive biofilms. Conductive biofilms are the basis of emerging technologies such as Microbial Fuel Cells and Microbial Electrosynthesis which are promising means to mitigate climate change and ensure security and access to clean water and feedstock chemicals upon which the production of most consumer goods depends. While the establishment of distinct phenotypic lineages and division of labor has been observed in conductive biofilms, little is known about how environmental fluctuations influence this process. Electroactive bacteria are ideal organisms for the exploration of general questions concerning how bacteria model and respond to environmental fluctuations due to the ability to control their redox environment by modulating the voltage of electrodes to which they are electrochemically connected. The following is a report on the development status of a stochastic model of electroactive bacteria responding to environmental fluctuations and corresponding experiments. The long-term goal is to determine if and how predictability of the local redox environment affects the epigenome of electroactive bacteria, how this determines their phenotypic distribution, maximal expected log-growth rate, and to use these findings to improve the design of microbial electrochemical technologies. Such a project has the potential to not only improve performance of technologies based on electroactive microbes, but to test theoretical results from computational mechanics concerning information processes in bacteria.

## **Introduction**

The current water-energy-food-climate (WEFC) system is unsustainable given humanities current modes of production, consumption, and resource stewardship [1]. A related crisis facing modernized economies is the exhaustion of fossil-fuel based feedstock chemicals currently relied upon for the production of plastics, rubber, textiles, and a wide variety of other goods and materials [2]. The use of biomass derived feedstocks as substitutes for fossil fuels competes for land and food production, exacerbating the stress upon the WEFC system. Inventive technological solutions are needed to mitigate looming crises as the effects of resource scarcity and climate change manifest themselves. Microbial Electrochemical Technologies (METs) are among the most promising solutions to confront problems facing the WEFC system. Microbial electrochemical technologies represent a new paradigm for the production of energy, fuels, chemicals, and sources of protein from waste streams. Wastewater treatment plants are particularly attractive sites for incorporation of these technologies due to their ability to act as resource banks from which these fuels, chemicals, and proteins can be manufactured, with the possibility to power these processes through onsite energy generation from wastewater [3]. Wastewater treatment plants can not only supplement or partially replace crucial resource supply chains that currently have negative impacts on the WEFC system due to their source of their feedstocks, but can simultaneously offset the much of the energy consumption and greenhouse gas emissions wastewater treatment itself is responsible for.

The basis of METs are electroactive bacteria capable of direct electron transfer with electrodes. A great deal of physiological and genomic information about model electroactive bacteria has been gained in recent decades [4]. However, much remains unknown about how sensory and information processes govern their behavior in response to environmental fluctuations in redox conditions, pH, temperature, and other environmental variables. Gaps in knowledge range from how their redox sensory apparatuses work to determining how such organisms internalize memories or models of the fluctuations in their local environment, and how these information processes affect or are affected by intracellular redox states. Within the field of biology there is also a need to incorporate quantitative frameworks to qualify notions such as “environmental predictability” from the perspective of bacteria. These topics are an active area of research in information thermodynamics and computational mechanics. Recent literature from these fields has proposed models of how stochastic fluctuations affect the operations of sensors and biological systems, as well as how cells store and process environmental information [5-8]. There is relatively little in terms of experimental validation of these models, however. Therefore model systems for which the environment can be well defined and controlled are desirable. In this report electroactive bacteria are proposed to be ideal model organisms for such studies, to both improve METs and answer fundamental questions about bacterial information processing of environmental data. In what follows, progress on a stochastic model of a single cell which takes environmental inputs from epsilon machines with well characterized statistics is introduced.

## **Biological Redox Chemistry and Electroactive Bacteria**

Among all the fundamental processes of cellular biology, oxidation-reduction (“redox”) reactions from which cells obtain energy are one of the most vital. Life has been described as having to fight a constant battle against the second law of thermodynamics via maintenance of non-equilibrium states [9]. This is

made possible by coupling chemical reactions through the uptake of reduced (electron rich) organic or inorganic molecules, utilizing these electrons to power manifold cellular processes, and donating the used electrons to terminal, oxidized acceptor molecules, such as oxygen, sulfate, or nitrate. The chemical potential difference between electron donors and electron acceptors provides the thermodynamic driving force that powers all life. As depicted below in Figure 1, electron donor molecules such as glucose or hydrogen diffuse into cells where enzymes liberate their electrons to power intracellular processes, until they are taken up by terminal electron acceptor molecules, such as sulfate, which enter and exit cells via diffusion or active pumping across the cellular membrane.

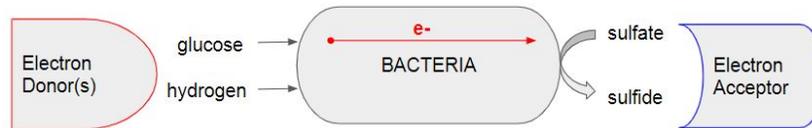


**Figure 1.** Generic schematic of bacterial redox processes that power cells.

In recent decades *electroactive bacteria* capable of electron transfer outside the cell via non-diffusive mechanisms have been the subject of intense research. Electroactive bacteria are capable of electron transfer with terminal electron acceptors or donors that reside outside of their cell bodies via novel molecular mechanisms which have only been resolved in a handful of model organisms [4, 10]. Two direct and two indirect electron transfer pathways have been found to mediate these external electron transfer processes, as depicted in Figure 2 below.

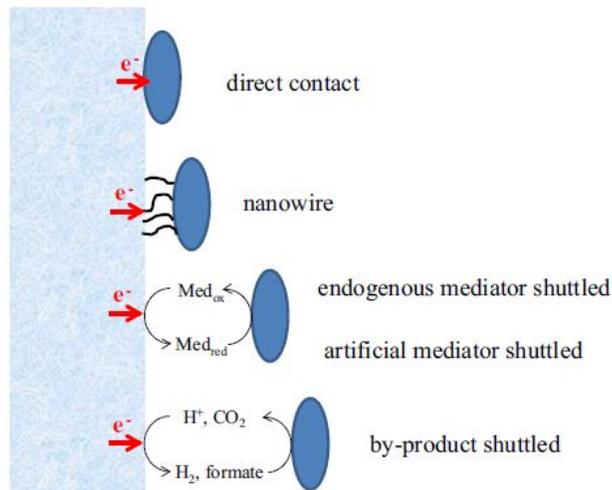


**Figure 2.** Electroautotrophic bacteria with electron transfer from cathode via four distinct mechanisms [11].

There are two types of electroactive bacteria: exoelectrogens and electroautotrophs. Exoelectrogens are microbes that use external terminal electron *acceptors* for respiration, such as an anode (an electrode with a positively poised voltage) or minerals. Electroautotrophs utilize external electron *donors* such as cathodes (an electrode with negatively poised voltage), metals such as steel, or reduced minerals. Exoelectrogens are responsible for the electrical power produced by Microbial Fuel Cells (MFCs). As with chemical fuel cells, in MFCs fuel in the form of reduced organic compounds (i.e. wastewater) is fed

into an electrochemical chamber with an anode covered in a biofilm consisting of exoelectrogens. These exoelectrogens oxidize the reduced organic compounds and respire these organically derived electrons on to the external anode to complete their electron transport processes. The electrical current/voltage produced from this process can be used to power an external load. Theoretical calculations indicate the energy contained in wastewater is several times greater than the total power requirements for treatment processes [3]. Electroautotrophs are used in a process called Microbial Electrosynthesis (ME) for the production of fuels, chemicals, or single cell proteins from  $\text{CO}_2$  and electricity. In this process a biofilm containing electroautotrophs grows on the surface of a cathode as seen in Figure 3 below. The microbes in the biofilm obtain energy via uptake of electrons from the cathode and use  $\text{CO}_2$  as their carbon source to synthesize commodity chemicals or biodegradable plastics. This technology is still in the research and development phase and is not yet competitive with legacy chemical manufacturing. Controlling the internal redox states of cells and phenotypic variation within biofilms is desirable to optimize both types of METs [3,4].

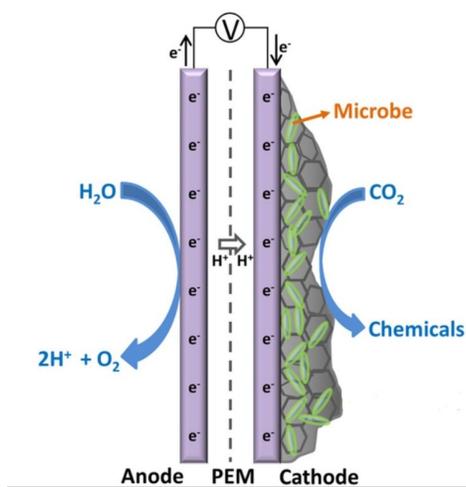


Figure 3. Microbial Electrosynthesis Cell [12].

From the perspective of bacteria, phenotypic variation within monocultures is a form of “bet hedging” that can maximize growth rates. Instances of phenotypic variation, such as metabolic stratification, have been observed in conductive biofilms growing on electrodes [13]. For both MFCs and ME, control of phenotypic variation or growth rates can improve system performance. As such, understanding the underlying dynamics of these processes would be enormously informative for engineering MET systems. Marzen and Crutchfield (2018) developed a model for how bacteria retain memories of environmental fluctuations and optimal strategies for tuning phenotype in response [8]. Within their framework environmental fluctuations are modeled as a stationary stochastic process. Environmental states are observable by bacteria via a sensor, and the “realizable epigenetic memories...are the causal states of the observed environment.” The “value of information” stored in epigenetic memories is measured by an increase in the maximal expected log-growth rate,  $\Delta r^*$ , of the bacterial population, above the maximal expected growth rate for a bacterial population with no epigenetic memory. The quantity  $\Delta r^*$  can be calculated as the mutual information between the current environmental state ( $X_t$ ) and the previous epigenetic state ( $Y_{t-1}$ ), given in equation 1 below [8].

$$\Delta r^* = I[Y_{t-1}; X_t] \quad (1)$$

The quantity on the RHS of equation 1 is known as the instantaneous predictive information. From the data processing inequality:  $I[Y_{t-1}; X_t] \leq I[X_{-\infty:t}; X_t]$ . Where  $I[X_{-\infty:t}; X_t] = H[X_t] - h_\mu$  is the “predicted information rate...largely controlled by the environment’s intrinsic randomness”, i.e. the Shannon entropy rate,  $h_\mu$  [8]. Based on these results, an upper bound on the increase in max expected log-growth can be computed for a given finite state epsilon machine that generates the environmental states  $X_t$ .

In the context of experiments involving electroactive bacteria,  $H[X_t] - h_\mu$  can be controlled by the experimentalist via the electrode, so long as time steps are not shorter than typical response times of potentiostat control circuits (~microseconds). Therefore it is conceivable that the model introduced by Marzen and Crutchfield could be emulated by experimental control of an environmental variable, electrode voltage, while others are held constant. Furthermore a particular type of epigenetic memory, DNA methylation, could be measured for a population of bacteria subjected to a voltage control protocol generated by an epsilon machine with well-defined statistics [14]. Using epsilon machines with different  $H[X_t] - h_\mu$  values should lead to observable differences in  $\Delta r^*$  and epigenetic memory.

It is suggested that the model of Marzen and Crutchfield be modified or perhaps extended to a scenario where a sensor is not the mediator between environmental and epigenetic states. Instead, the intracellular redox state of a cell could serve as the intermediary. Intracellular redox states are directly correlated with fluctuations in the local redox environment in terms of the identity and quantity of electron donors and/or acceptors, and have a significant influence over epigenetic processes [15]. In what follows the general model to simulate the intracellular redox state of an electroactive microbe is considered. Progress on the development of this model is provided for a simple case, and future work is outlined.

### **Dynamical system**

For this project the dynamical system is the intracellular redox states of a single bacterial cell, depicted in Figure 4. This model was adapted from a stochastic queuing model developed by Michelusi et al. [16]. Michelusi et al. explicitly attempted to model chain-forming electroactive bacteria capable of accepting and donating electrons via external electron transfer. Their model captures the time evolution of important redox molecule (NADH & ATP) concentrations involved in bacterial electron transport chains given different environmental redox scenarios (types and concentration profiles of electron donors/acceptors). Their model was validated using time series data of intracellular concentrations of NADH and ATP in yeast under specific electron acceptor/donor constraints. Such data sets were and still are not available for electroactive bacteria, so their use of yeast data was to validate a simpler, sub-set of their model for which the underlying cellular processes are the same for both organisms. This allowed them to approximate numeric coefficients needed for the model, which are also used for the simulations in this report [16].

The time evolution of this single cell model depends on the concentration profiles of each pool, the flow rates into and out of pools, and the external redox environment. In this report two scenarios for the redox environment were simulated; one in which the external environment is constant and another for which a

bit string representing environmental fluctuations was generated from the epsilon machine for a biased coin. The bit string generated by the biased coin HMM was used as input for the environmental variable of which the internal cellular state is a function. In what follows the general model for an electroautotrophic bacteria is introduced, along with the relevant equations and matrices that govern the behavior of the system. The special case simulated for this project is then detailed in the methods section, and the results of simulations and commentary on future work is provided.

The most general model consists of three, time dependent intracellular redox pools. Figure 4 shows these three pools, the variables for their time dependent state values, as well as flow rates in and out of each pool. In this model electrons can enter the cell through diffusion of electron rich molecules, “ED”, (shown as middle pool) or from an electrode, “ET from electrode”, (left pool). Electrons stored in both the Internal Carrier Pool (IECP) and the External Membrane Electron Pool (EMEP) are used to power the electron transport chain of the cell, which in turn results in a proton concentration gradient across the cell’s inner membrane. This proton gradient powers the synthesis of ATP molecules, which are used as an energy source for a variety of cellular processes. This cell model captures the basic sources and pathways of electrons within a cell. A queuing model is used which increments or decrements the value for a given pool by one “unit” per iteration, based on allowed transitions between states.

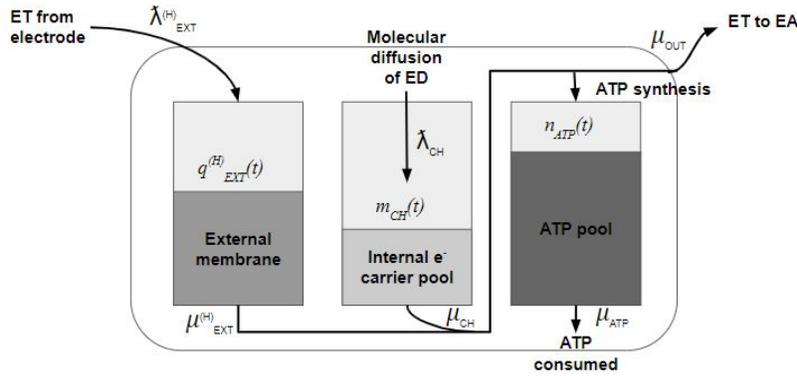


**Figure 4.** General model for bacterial intracellular redox pools and associated inflow and outflow rates.

1. The External Membrane Electron Pool (EMEP):  $q_{EXT}(t) \in \mathcal{Q}_{EXT} = \{0,1,2,3,\dots,M_{EXT}\}$  where  $M_{EXT}$  represents the electron storage capacity of proteins such as c-type cytochromes which can accept high energy electrons from external donors, such as an electrode. Flows into and out of this electron pool are given by  $\lambda_{EXT}^{(H)}$  and  $\mu_{EXT}^{(H)}$ , respectively. The electrons from this pool flow into the ATP pool to synthesize ATP molecules.
2. The Internal Electron Carrier Pool (IECP):  $m_{CH}(t) \in \mathcal{M}_{CH} = \{0,1,2,3,\dots,M_{CH}\}$ , where  $M_{CH}$  is the electrochemical storage capacity of the cell. This pool represents the number of molecules, such as NADH, which act as general purpose, diffusible electron reserves within the cell. Diffusible molecules that act as electron donors, such as acetate or hydrogen, enter the cell (ED in Figure 4) and the electrons are converted to NADH and collected in the IECP. Electrons from this pool

leave (decrement) when they are used to synthesize an ATP molecule.  $\lambda_{CH}$  and  $\mu_{CH}$  represent flow rates in and out of the IECP, respectively.

3. The ATP pool:  $n_{ATP}(t) \in \mathcal{N}_{AXP} = \{0, 1, 2, 3, \dots, N_{AXP}\}$ , where  $N_{AXP}$  is the ATP storage capacity of the ATP pool. ATP molecules are the general energy source within the cell and electrons from either the IECP or EMEP are used to synthesize ATP.  $\mu_{ATP}$  is the rate at which ATP molecules are used by the cell, after which electrons are taken up by the terminal electron acceptor at a rate  $\mu_{OUT}$ . The rate at which ATP molecules are synthesized is determined by the electron flow rates into the pool from both the IECP and EMEP,  $\mu_{CH} + \mu_{EXT}^{(H)}$ .

The internal state equation for the single cell and the state space, respectively, are provided below:

$$s_i(t) = (m_{CH}(t), n_{ATP}(t), q_{EXT}(t)) \quad (2)$$

$$\mathcal{S}_i = \mathcal{M}_{CH} \times \mathcal{N}_{AXP} \times \mathcal{Q}_{EXT} \cup \{\text{DEAD}\} \quad (3)$$

The environmental state is modeled as  $s_E(t) = (\theta_D(t), \theta_A(t))$ , where  $\theta_D(t)$ ,  $\theta_A(t)$  are the concentration of terminal electron donors and acceptors, respectively.

The state distribution of the system at some time  $t > 0$  is determined by the probability transition matrix for the discrete Markov chain between cell states, denoted  $\mathbf{P}_t$ , and has  $(|\mathcal{S}_i| - 1) \times (|\mathcal{S}_i| - 1)$  elements, but due to the queuing properties, only a subset of transitions are allowed, such that for systems with  $M_{CH} = N_{AXP} > 1$ ,  $\mathbf{P}_t$  is a sparse matrix. The method to calculate  $\mathbf{P}_t$  is detailed in the methods section for the specific simulations used for this report.

To incorporate a structured environmental input into this model for which information theoretic quantities can be calculated, an epsilon machine was used to generate bit-strings. The environmental variable,  $s_E(t)$ , took on piecewise constant values for each random time interval of the simulation according to these previously generated bit strings. As detailed in the methods sections, the flow rates are dependent on the environmental state  $s_E(t)$ . In this way the statistics of the intracellular redox states is partly determined by the environment state variable. The epsilon machine for a biased coin was used for the simulations in this report since its statistical properties can be tuned by varying the bias. Given the binary alphabet ( $\mathbf{A} = \{0, 1\}$ ), the physical interpretation is that the ED is not available for a bit value of 0 ( $0 \rightarrow s_E(t) = 0$  mM) or the ED is available at a fixed concentration for a bit value of 1 ( $1 \rightarrow s_E(t) = 10$  mM). Though it is left to future work, if the ED were the cathode this value would be expressed as a voltage rather than concentration.

## Methods

For this report the three pool model was simplified to two-pools,  $s_i(t) = (m_{CH}(t), n_{ATP}(t))$ , as shown below in Figure 6. As stated in Michelusi et al. (2014), there is no published data available to estimate parameters needed to calculate reaction rates for the EMEP. Therefore the simulations reported here also considered diffusible EDs and made use of the parameter values reported by Michelusi et al.

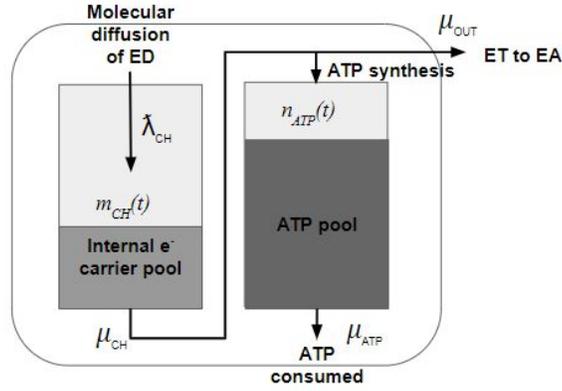


**Figure 5.** Simplified two-pool cell mode,  $s_i(t) = (m_{CH}(t), n_{ATP}(t))$ , used for simulations.

The internal state equation for the single cell is:  $s_i(t) = (m_{CH}(t), n_{ATP}(t))$ , with state space  $\mathcal{S}_1 = \mathcal{M}_{CH} \times \mathcal{N}_{ATP} \cup \{\text{DEAD}\}$ . For the purpose of constructing a simple model the IECP and ATP pool values were kept small ( $M_{CH} = N_{ATP} = 2$ ). This results in a 9 state system as depicted in Figure 6 below, along with allowed transitions between these states based on the properties of the queue.

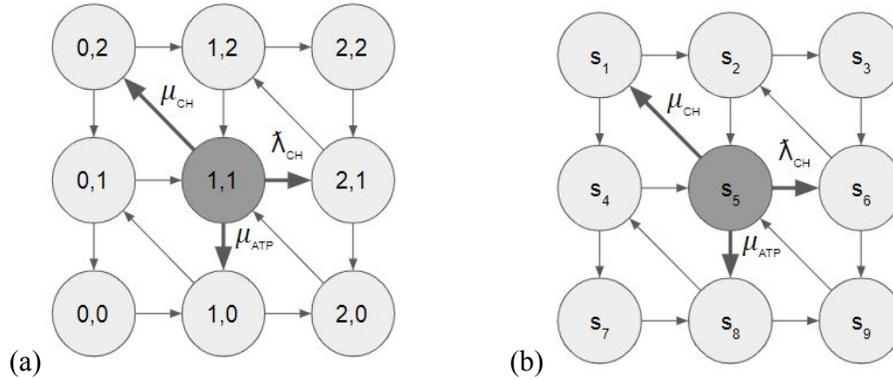


**Figure 6.** (a) Markov chain for two pool model,  $s_i(t) = (m_{CH}(t), n_{ATP}(t))$ , where  $M_{CH} = N_{ATP} = 2$ . Allowed state-to-state transitions based on queuing rules are depicted by directed arrows, with associated transition rates shown for  $s_i = (1, 1)$  & (b) the same model with states labelled for construction of matrices  $\mathbf{P}$  &  $\mathbf{R}$ .

For this model the cardinality of the transition probability matrix is  $|\mathbf{P}| = (|\mathcal{S}_1| - 1) \times (|\mathcal{S}_1| - 1) = 9 \times 9 = 81$ , and has 16 non-zero entries.

To determine the state-to-state time evolution of the system a transition probability matrix for some time  $t > 0$ ,  $\mathbf{P}_t$ , can be calculated from  $\mathbf{P}_t = \exp\{\mathbf{A}t\}$ , where  $\mathbf{A} = \mathbf{R}(\mathbf{P} - \mathbf{I})$ .  $\mathbf{P}$  is the probability transition matrix for the discrete Markov chain between cell states, and  $\mathbf{R}$ , is the rate matrix, a diagonal matrix where  $\mathbf{R}(i, i) = R_i$ , and  $R_i = \sum_s \lambda_{i,s}$ , and  $\mathbf{I}$  is the identity matrix [16]. The  $\mathbf{R}$  and  $\mathbf{P}$  matrices used for simulations are provided below along with explicit examples of their entries for clarity.



$$\mathbf{R} = \begin{pmatrix} R_1 & 0 & 0 & 0 & 0 & 0 & 0 & 0 & 0 \\ 0 & R_2 & 0 & 0 & 0 & 0 & 0 & 0 & 0 \\ 0 & 0 & R_3 & 0 & 0 & 0 & 0 & 0 & 0 \\ 0 & 0 & 0 & R_4 & 0 & 0 & 0 & 0 & 0 \\ 0 & 0 & 0 & 0 & R_5 & 0 & 0 & 0 & 0 \\ 0 & 0 & 0 & 0 & 0 & R_6 & 0 & 0 & 0 \\ 0 & 0 & 0 & 0 & 0 & 0 & R_7 & 0 & 0 \\ 0 & 0 & 0 & 0 & 0 & 0 & 0 & R_8 & 0 \\ 0 & 0 & 0 & 0 & 0 & 0 & 0 & 0 & R_9 \end{pmatrix}$$

**Figure 7.** Rate matrix,  $\mathbf{R}$ , used for simulations.

Where  $R_i = \sum_s \lambda_{i,s}$ , and  $\lambda_{i,s}$  represents a general rate term from current state  $i$ , to some new state,  $s$ . For example, based on the allowed transitions in Figure 6 above,  $\mathbf{R}_1 = \lambda_{(\text{CH})1,2} + \mu_{(\text{ATP})1,4}$ .

$$\mathbf{P} = \begin{pmatrix} 0 & p_{1,2} & 0 & p_{1,4} & 0 & 0 & 0 & 0 & 0 \\ 0 & 0 & p_{2,3} & 0 & p_{2,5} & 0 & 0 & 0 & 0 \\ 0 & 0 & 0 & 0 & 0 & p_{3,6} & 0 & 0 & 0 \\ 0 & 0 & 0 & 0 & p_{4,5} & 0 & p_{4,7} & 0 & 0 \\ p_{5,1} & 0 & 0 & 0 & 0 & p_{5,6} & 0 & p_{5,8} & 0 \\ 0 & p_{6,2} & 0 & 0 & 0 & 0 & 0 & 0 & p_{6,9} \\ 0 & 0 & 0 & 0 & 0 & 0 & 0 & p_{7,8} & 0 \\ 0 & 0 & 0 & p_{8,4} & 0 & 0 & 0 & 0 & p_{8,9} \\ 0 & 0 & 0 & 0 & p_{9,5} & 0 & 0 & 0 & 0 \end{pmatrix}$$

**Figure 8.** Transition probability matrix,  $\mathbf{P}$ , used for simulations.

Where entries in  $\mathbf{P}(i,j)$  are calculated as  $\lambda_{i,j} / R_i$ , where again  $\lambda_{i,j}$  is the transition rate for going from  $s_i$  to  $s_j$ , and  $R_i$  was previously defined as the sum of rate terms leaving a given state,  $s_i$ . For example,  $\mathbf{P}_{12} = \lambda_{(\text{CH})1,2} / (\lambda_{(\text{CH})1,2} + \mu_{(\text{ATP})1,4})$ . After constructing these two matrices the transition probability matrix for some time  $t > 0$ ,  $\mathbf{P}_t$ , can be calculated from  $\mathbf{P}_t = \exp\{\mathbf{A}t\}$ , where, again,  $\mathbf{A} = \mathbf{R}(\mathbf{P} - \mathbf{I})$ . The following equations were used to calculate numerical values for transition rates and the matrices:

$$\lambda_{\text{CH}}(\mathbf{s}_1(t); \mathbf{s}_E(t)) = \gamma \Theta_D(t) + \varrho(1 - m_{\text{CH}}(t) / M_{\text{CH}}) \Theta_D(t) \quad (4)$$

$$\mu_{\text{CH}}(\mathbf{s}_1(t); \mathbf{s}_E(t)) = \eta(1 - n_{\text{ATP}}(t) / N_{\text{AXP}}) \quad (5)$$

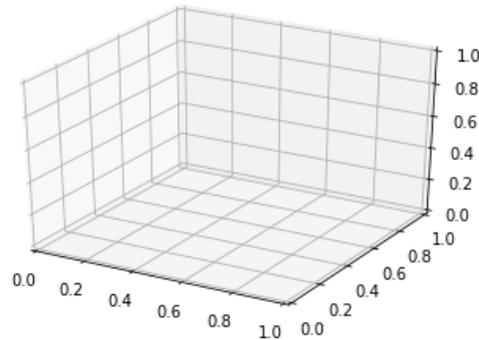
$$\mu_{\text{ATP}}(\mathbf{s}_1(t); \mathbf{s}_E(t)) = \beta \Theta_D(t) \quad (6)$$

Values for the parameters  $\gamma$ ,  $\varrho$ ,  $\eta$ ,  $\beta$  in equations 4-6 above were taken from Michelusi et al. [16]. The term  $\Theta_D(t)$  represents the electron donor concentration at time  $t$ , and provides the link between the bit string generated by the biased-coin epsilon machine. For example, assuming when EDs are present the concentration is equal to 10 mM, if the bit string generated by the biased coin HMM is: 0 1 1, then for the first time interval  $t_0 \rightarrow t_1$   $\Theta_D(t) = 0$ ,  $t_1 \rightarrow t_2$   $\Theta_D(t) = 10$ ,  $t_2 \rightarrow t_3$   $\Theta_D(t) = 10$ , and so on. All simulations were carried out using the python programming language along with several libraries, such as scipy, cmpy, and numpy. The Gillespie simulation algorithm was used, whereby after initialization of the system, random

numbers based on defined exponential distributions were used to both select the next time interval, and the event/reaction that occurred during that time interval.

## Results

In progress...



## Conclusion

In progress...

## References:

1. Simpson, G. B., & Jewitt, G. P. (2019). The development of the water-energy-food nexus as a framework for achieving resource security: A review. *Frontiers in Environmental Science*, 7, 8.
2. Claassens, N. J., Sánchez-Andrea, I., Sousa, D. Z., & Bar-Even, A. (2018). Towards sustainable feedstocks: A guide to electron donors for microbial carbon fixation. *Current opinion in biotechnology*, 50, 195-205.
3. Lu, L., Guest, J. S., Peters, C. A., Zhu, X., Rau, G. H., & Ren, Z. J. (2018). Wastewater treatment for carbon capture and utilization. *Nature Sustainability*, 1(12), 750-758.
4. Logan, B. E., Rossi, R., & Saikaly, P. E. (2019). Electroactive microorganisms in bioelectrochemical systems. *Nature Reviews Microbiology*, 17(5), 307-319.
5. Still, S., Sivak, D. A., Bell, A. J., & Crooks, G. E. (2012). Thermodynamics of prediction. *Physical review letters*, 109(12), 120604.
6. Hartich, D., Barato, A. C., & Seifert, U. (2016). Sensory capacity: An information theoretical measure of the performance of a sensor. *Physical Review E*, 93(2), 022116.

7. Marzen, S. E., & Crutchfield, J. P. (2020). Prediction and Dissipation in Nonequilibrium Molecular Sensors: Conditionally Markovian Channels Driven by Memoryful Environments. *Bulletin of mathematical biology*, 82(2), 25.
8. Marzen, S. E., & Crutchfield, J. P. (2018). Optimized bacteria are environmental prediction engines. *Physical Review E*, 98(1), 012408.
9. Schrödinger, E., & Penrose, R. (1992). *What is Life?: With Mind and Matter and Autobiographical Sketches* (Canto). Cambridge: Cambridge University Press.
10. El-Naggar, M. Y., & Finkel, S. E. (2013). Live wires. *Scientist*, 27(5), 38-43. - <https://www.the-scientist.com/features/live-wires-39406>
11. Choi, O., & Sang, B. I. (2016). Extracellular electron transfer from cathode to microbes: application for biofuel production. *Biotechnology for biofuels*, 9(1), 11.
12. Aryal, N., et al (2016). Enhanced microbial electrosynthesis with three-dimensional graphene functionalized cathodes fabricated via solvothermal synthesis. *Electrochimica Acta*, 217, 117-122.
13. Chadwick, G. L., Otero, F. J., Gralnick, J. A., Bond, D. R., & Orphan, V. J. (2019). NanoSIMS imaging reveals metabolic stratification within current-producing biofilms. *Proceedings of the National Academy of Sciences*, 116(41), 20716-20724.
14. Sánchez-Romero, M. A., Cota, I., & Casadesús, J. (2015). DNA methylation in bacteria: from the methyl group to the methylome. *Current opinion in microbiology*, 25, 9-16.
15. Cyr, A. R., & Domann, F. E. (2011). The redox basis of epigenetic modifications: from mechanisms to functional consequences. *Antioxidants & redox signaling*, 15(2), 551-589.
16. Michelusi, N., Pirbadian, S., El-Naggar, M. Y., & Mitra, U. (2014). A stochastic model for electron transfer in bacterial cables. *IEEE Journal on Selected Areas in Communications*, 32(12), 2402-2416.